Master thesis and internship[BR]- Master's thesis : STUDY OF AN ADVANCED TANDEM BLADE DESIGN FOR INCREASING THE OPERATING RANGE OF A LOW PRESSURE COMPRESSOR[BR]- Integration internship

Auteur : Anton Dobarro, David
Promoteur(s) : Hillewaert, Koen
Faculté : Faculté des Sciences appliquées
Diplôme : Cours supplémentaires destinés aux étudiants d'échange (Erasmus, ...)
Année académique : 2024-2025
URI/URL : http://hdl.handle.net/2268.2/22986

1 Appendix

1.1 Front Blade Shape Modification

The effect of altering the defining parameters of the geometry on the monitored parameters is shown in the following Figures. It may be appreciated that the initial considered range for the parameters is too large, thus not many conclusions may be drawn from the results.

In Figure 1, the effect of the chord scale on the flow physics is shown.

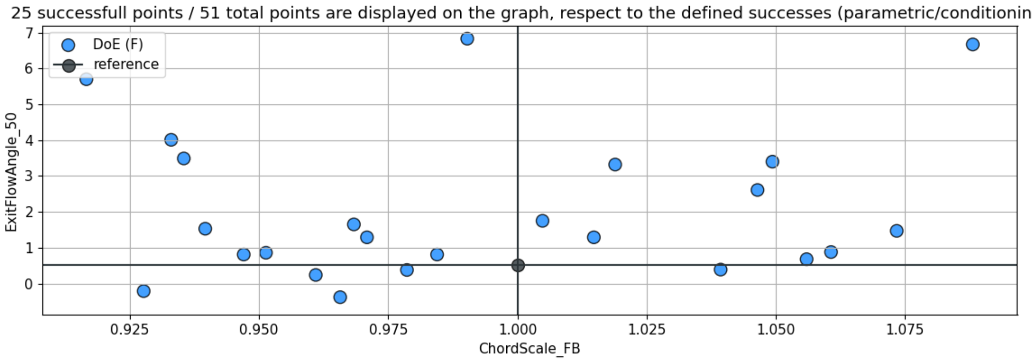

(a) Exit Flow Angle in terms of FB chord scale

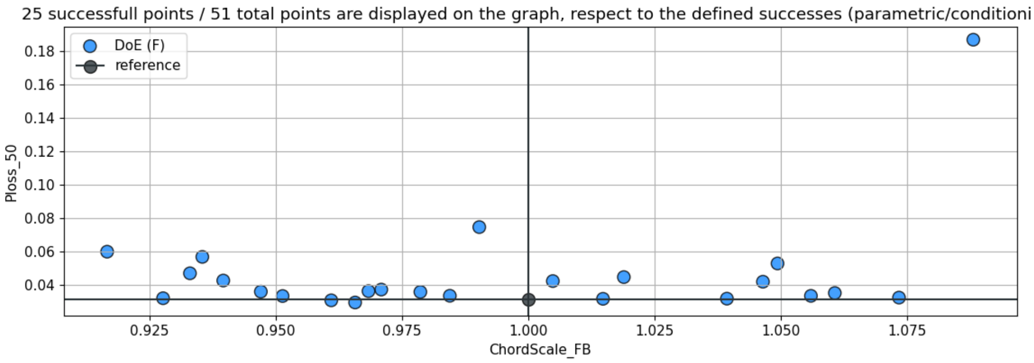

(b) ϕ in terms of FB chord scale

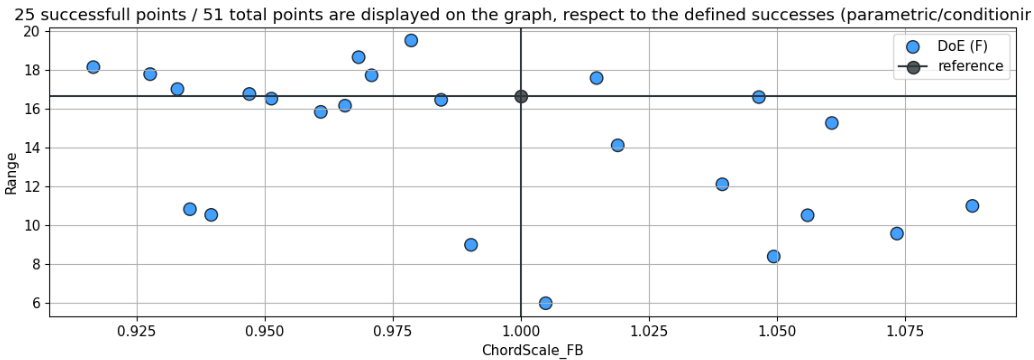

(c) Range in terms of FB chord scale

Figure 1. Effect of chord scale on flow physics

In Figure 2, the effect of the stagger angle on the flow physics is shown.

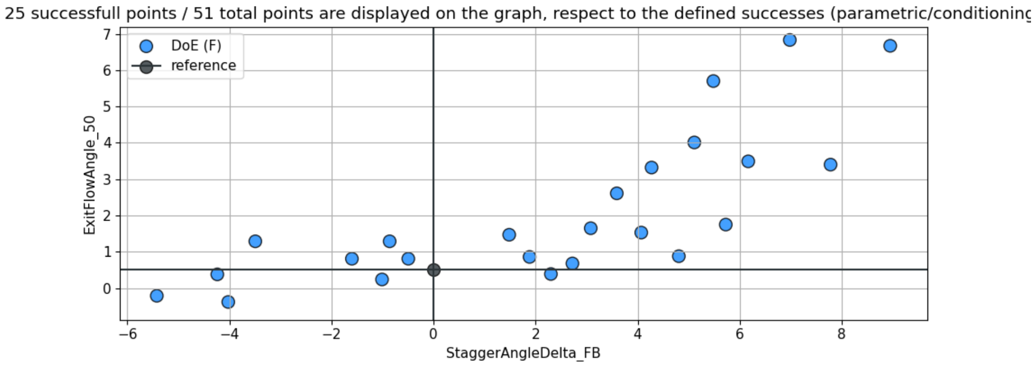

(a) Exit Flow Angle in terms of FB stagger deflection

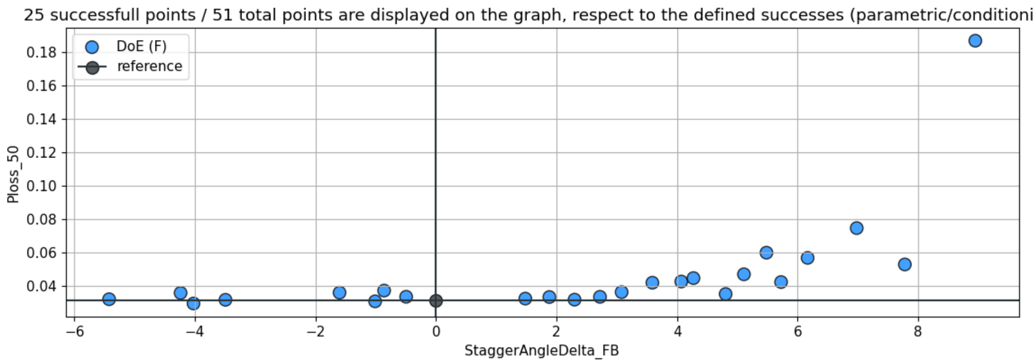

(b) ϕ in terms of FB stagger deflection

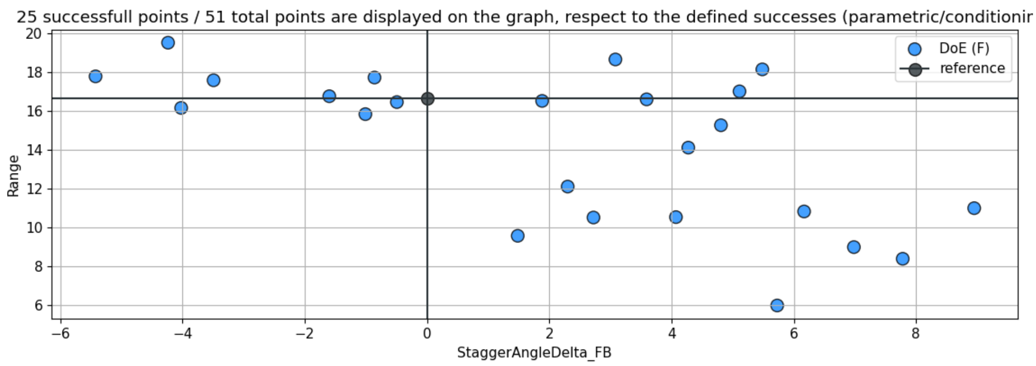

(c) Range in terms of FB stagger deflection

Figure 2. Effect of stagger deflection on flow physics

In Figure 3, the effect of the LE's angle deflection on the flow physics is shown.

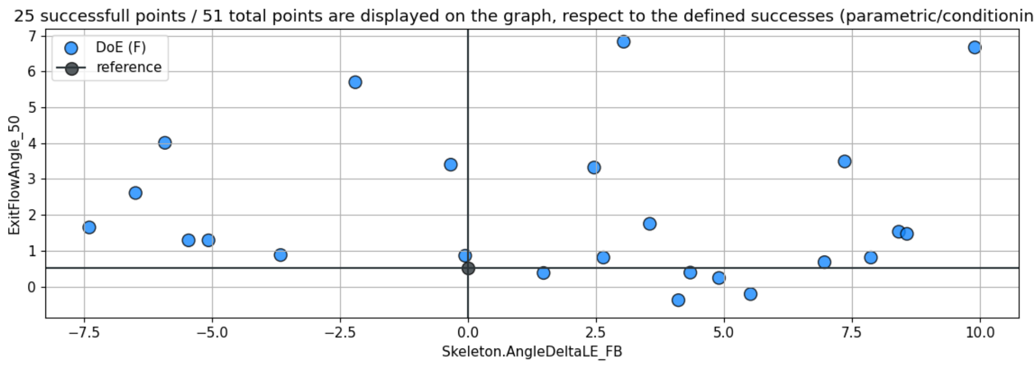

(a) Exit Flow Angle in terms of LE angle deflection

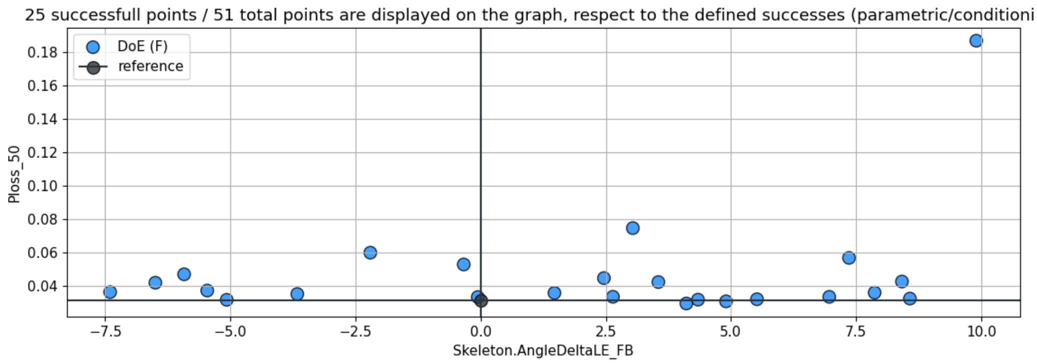

(b) ϕ in terms of LE angle deflection

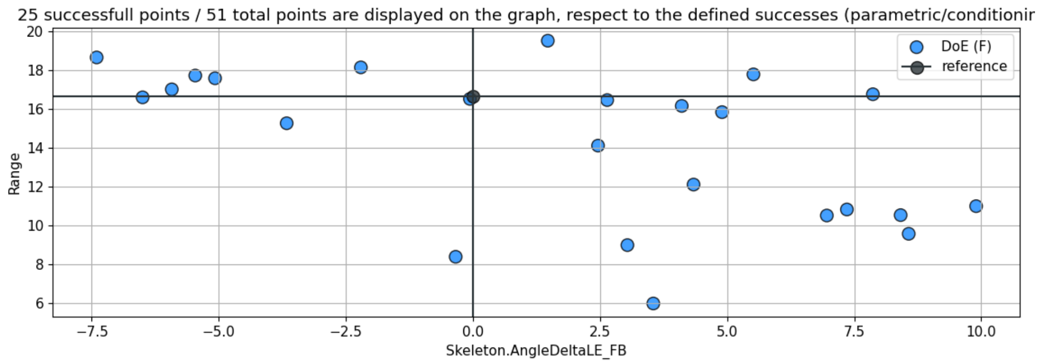

(c) Range in terms of LE angle deflection

Figure 3. Effect of LE angle deflection on flow physics

In Figure 4, the effect of the TE's angle deflection on the flow physics is shown.

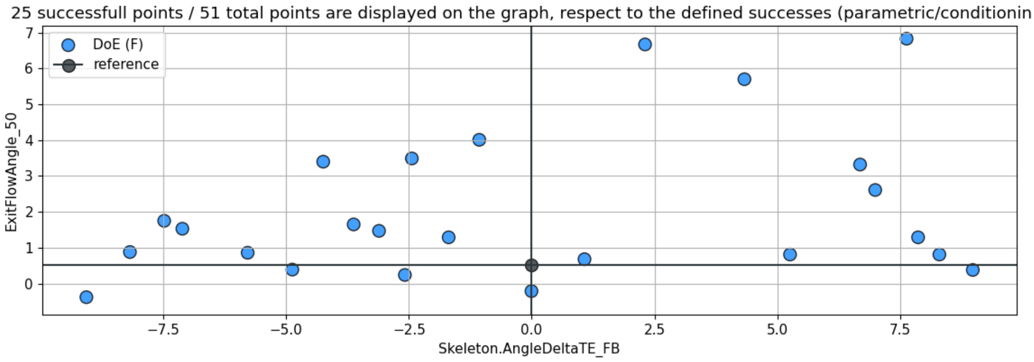

(a) Exit Flow Angle in terms of TE angle deflection

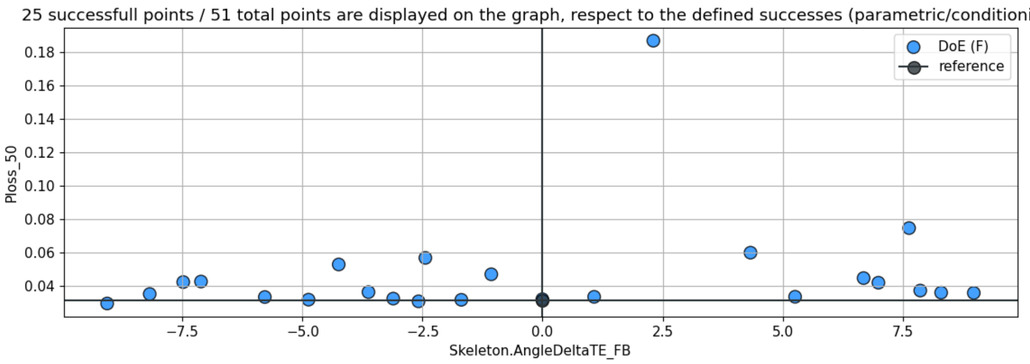

(b) ϕ in terms of TE angle deflection

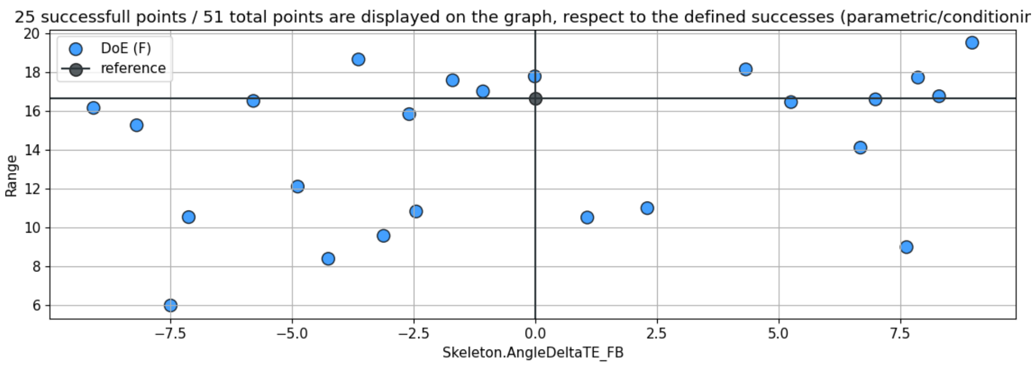

(c) Range in terms of TE angle deflection

Figure 4. Effect of TE angle deflection on flow physics

1.2 Rear Blade Shape Modification

In this section, an analysis similar to that which has been conducted on the FB is presented.

In Figure 5, it may be appreciated that even with a shift of 30% of the blade's thickness, the geometry does not vary that much. A similar conclusion may be drawn from the maximum thickness analysis. From Figure 6 it may be concluded that these parameters don't have a major influence on the physics of the flow. Thus, they have been ruled out as defining parameters of the optimization chain.

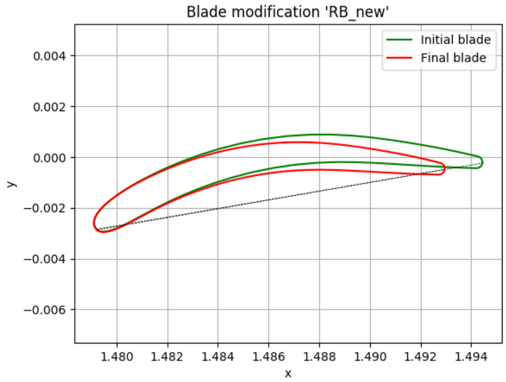

(a) RB comparison with -10% Chord Length

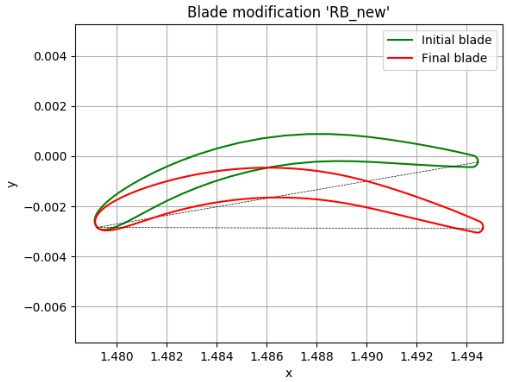

(b) RB comparison with -10º Stagger Angle

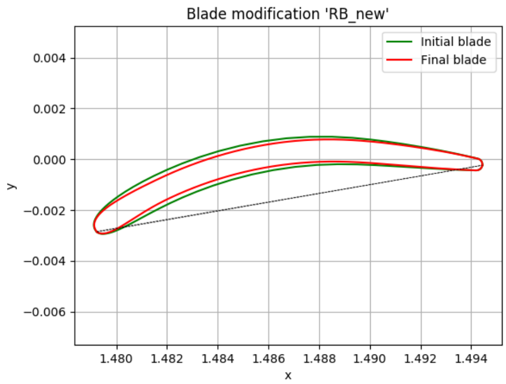

(c) RB comparison with -30% Thickness

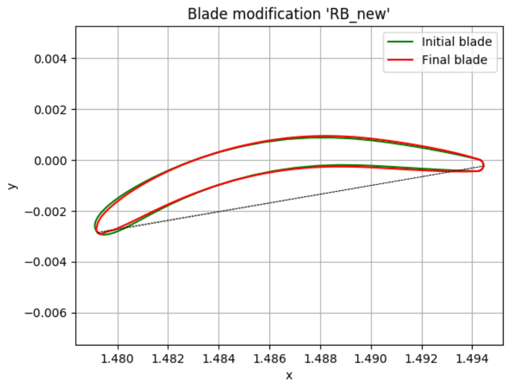

(d) RB comparison with +30% Thickness Shift

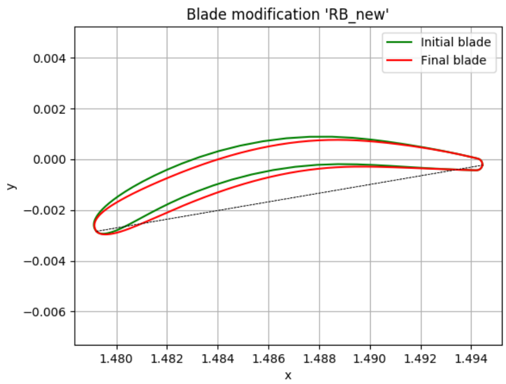

(e) RB comparison with -10º Metal Angle at LE

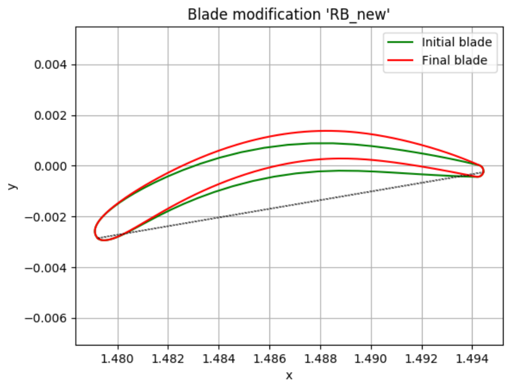

(f) RB comparison with -10º Metal Angle at TE

Figure 5. Rear Blade Shape modifications

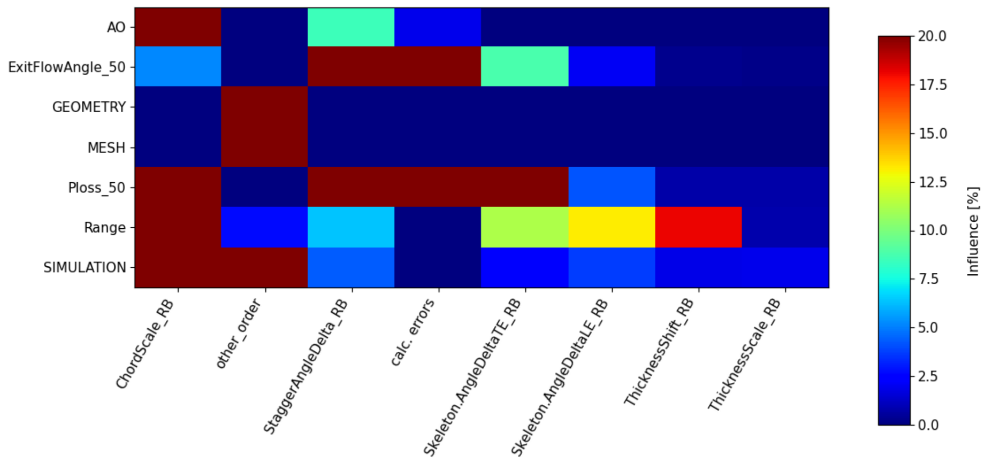

Figure 6. Global Sensitivity Analysis on Rear Blade

The effect of altering the defining parameters of the geometry on the monitored parameters is shown in the following Figures. It may be appreciated that the initial considered range for the parameters is too large, thus not many conclusions may be drawn from the results.

In Figure 7, the effect of the chord scale on the flow physics is shown.

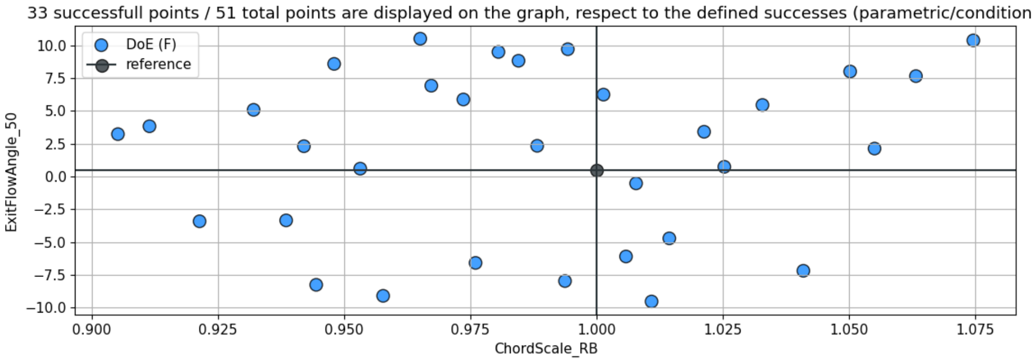

(a) Exit Flow Angle in terms of RB chord scale

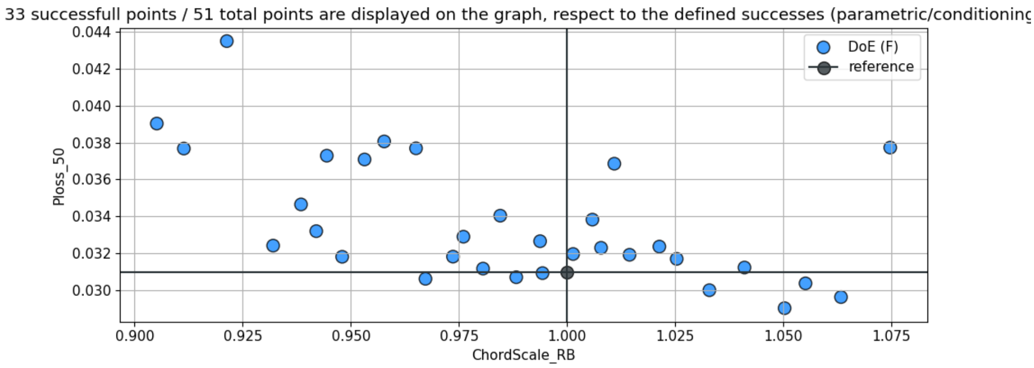

(b) ϕ in terms of RB chord scale

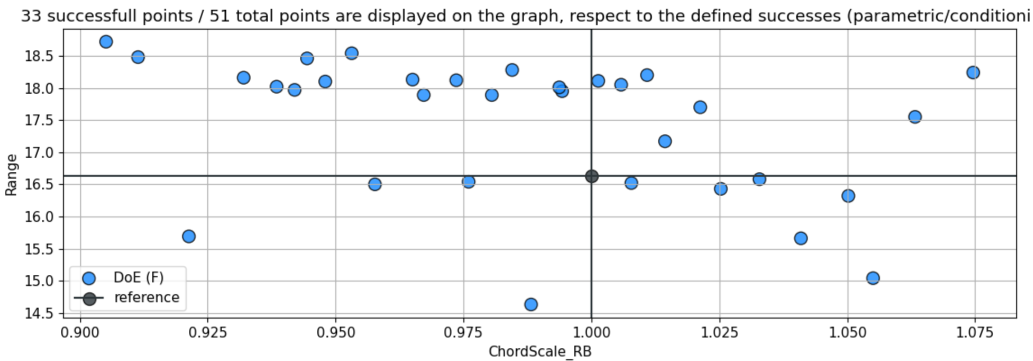

(c) Range in terms of RB chord scale

Figure 7. Effect of chord scale on flow physics

In Figure 8, the effect of the stagger angle on the flow physics is shown.

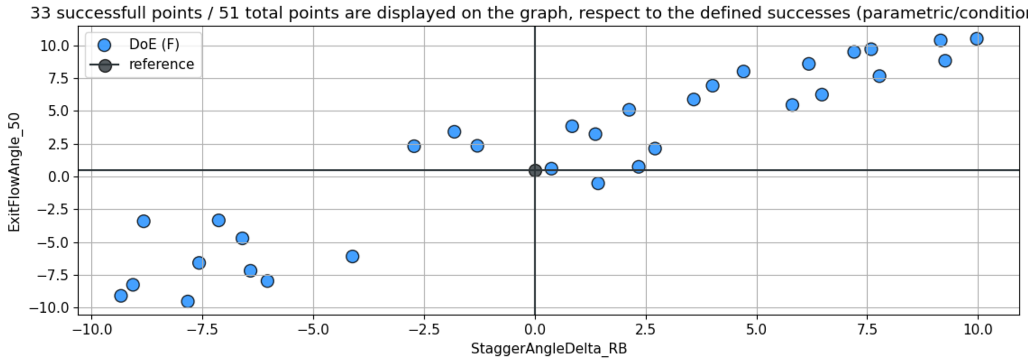

(a) Exit Flow Angle in terms of RB stagger deflection

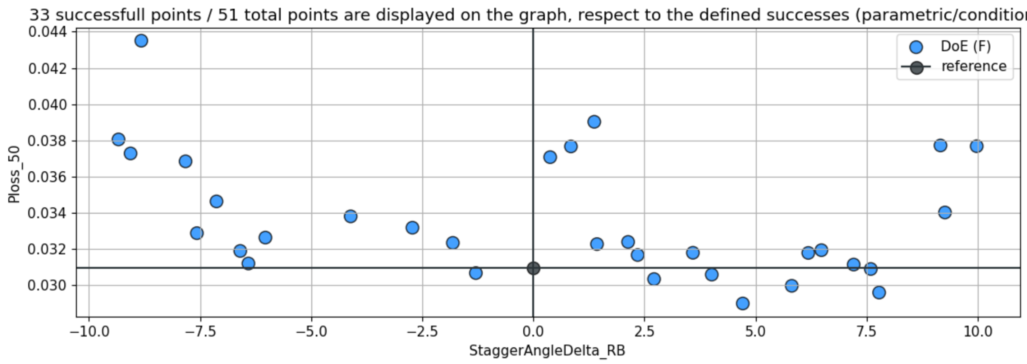

(b) ϕ in terms of RB stagger deflection

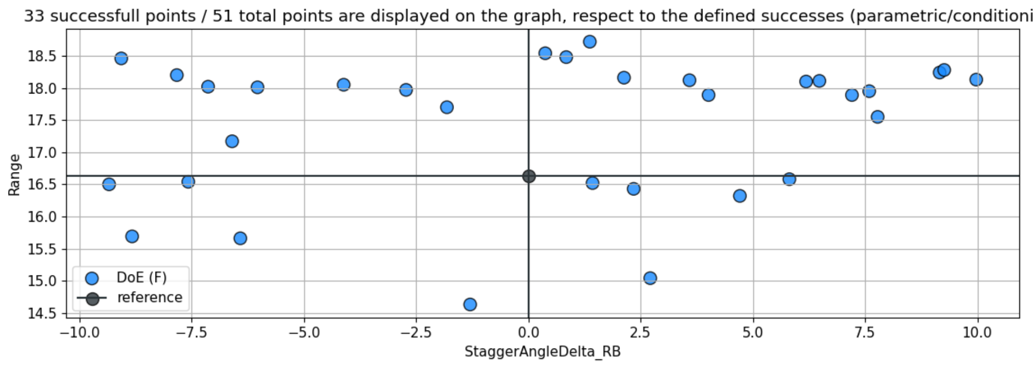

(c) Range in terms of RB stagger deflection

Figure 8. Effect of stagger deflection on flow physics

In Figure 9, the effect of the LE's angle deflection on the flow physics is shown.

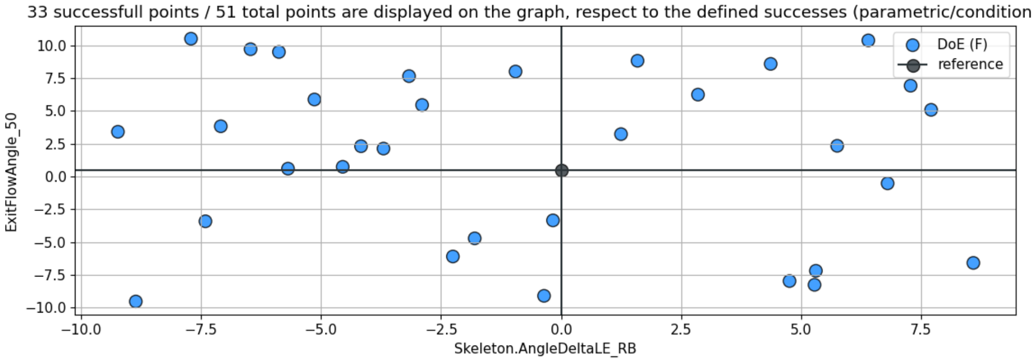

(a) Exit Flow Angle in terms of LE angle deflection

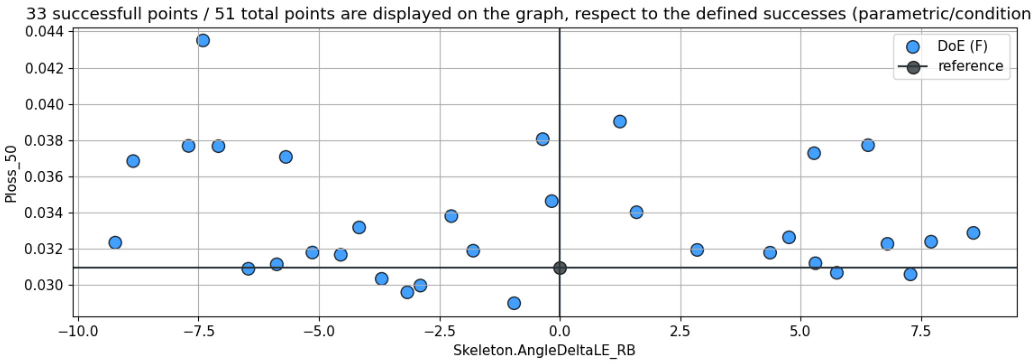

(b) ϕ in terms of LE angle deflection

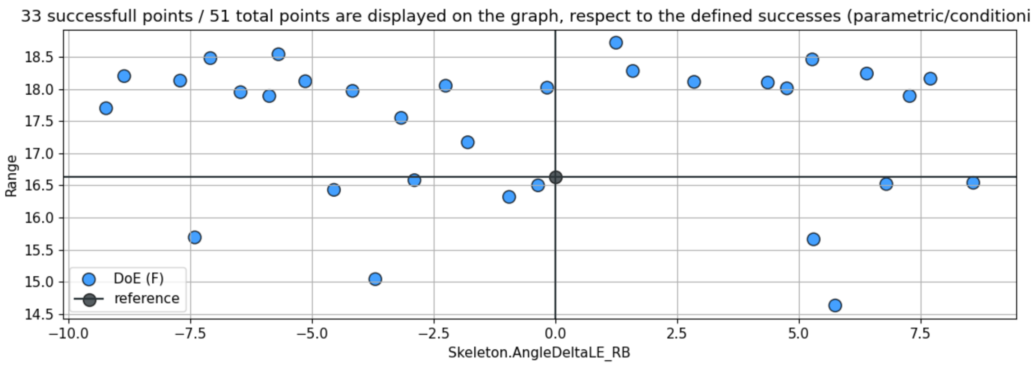

(c) Range in terms of TE angle deflection

Figure 9. Effect of LE angle deflection on flow physics

In Figure 10, the effect of the TE's angle deflection on the flow physics is shown.

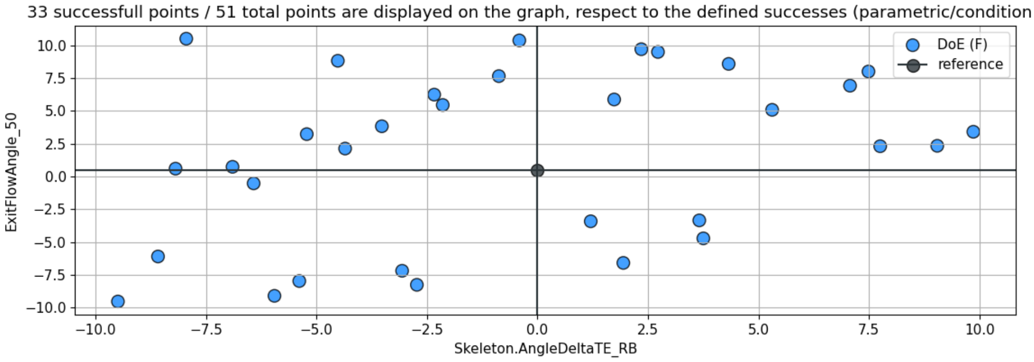

(a) Exit Flow Angle in terms of TE angle deflection

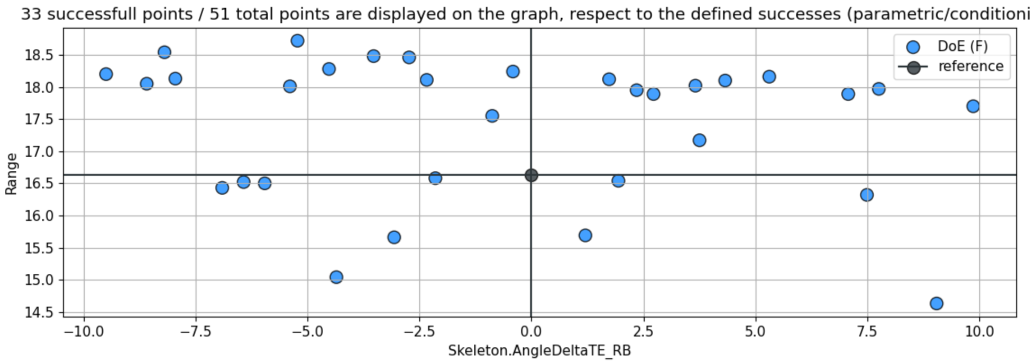

(b) ϕ in terms of TE angle deflection

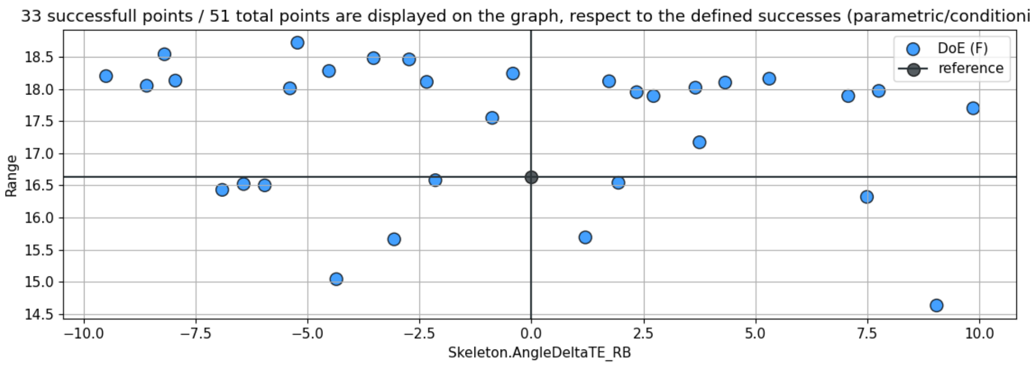

(c) Range in terms of TE angle deflection

Figure 10. Effect of TE angle deflection on flow physics

1.3 Performance Optimization

The results of the first optimization are presented in this section.

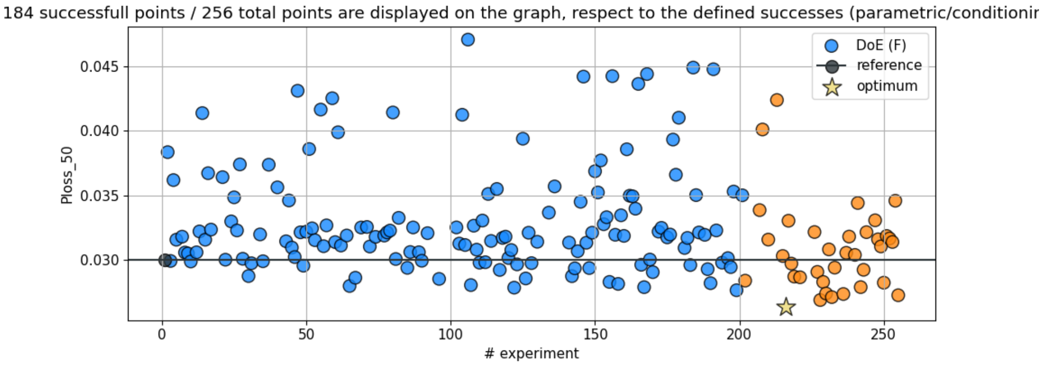

(a) Pressure losses

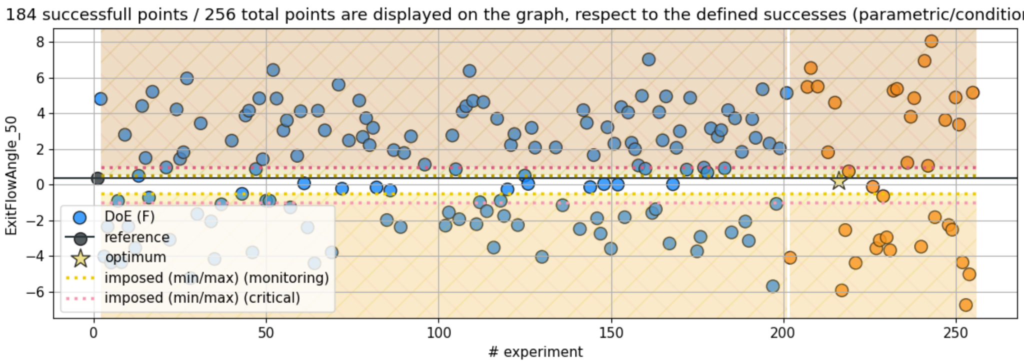

(b) Exit flow angle

Figure 11. Performance of flow quantities of the test cases

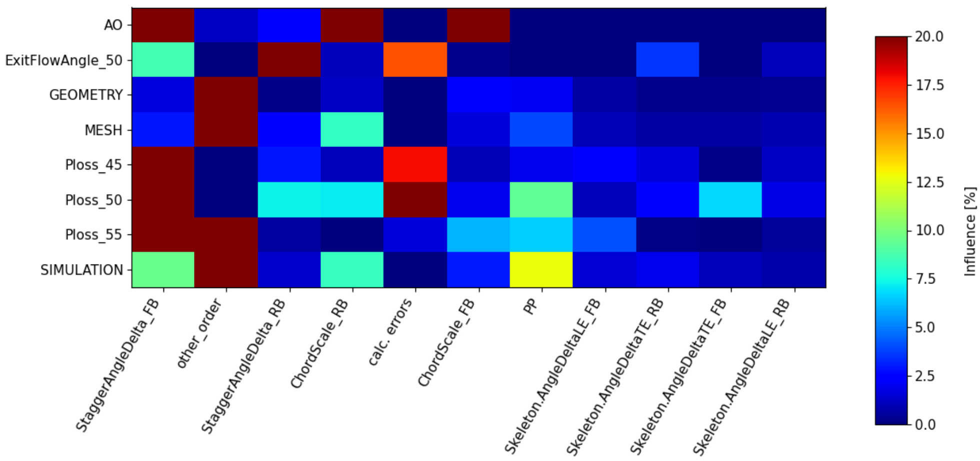

Figure 12. Global Sensitivity Analysis of the optimization

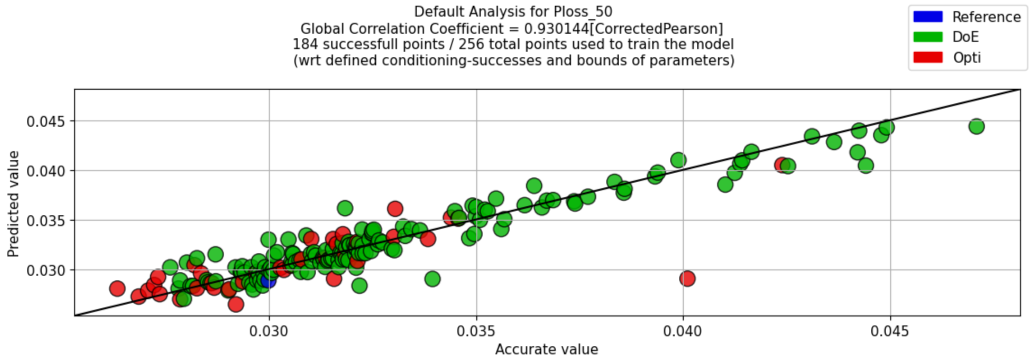

(a) Pressure losses

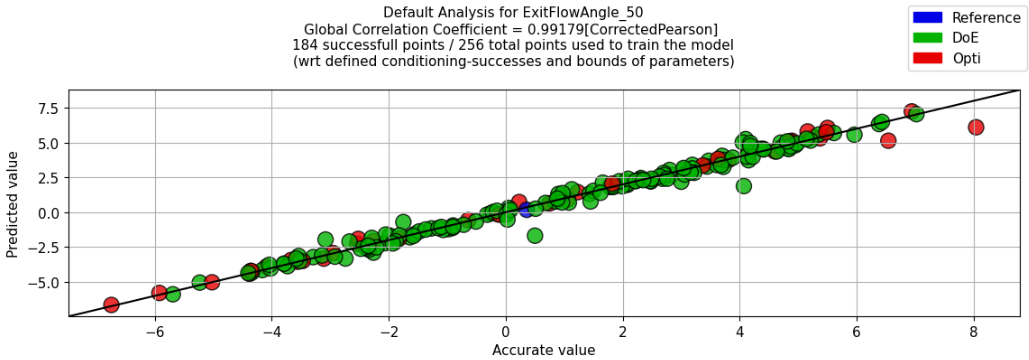

(b) Exit flow angle

Figure 13. Model quality of flow quantities of the test cases

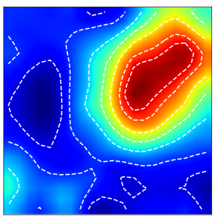

(a) Pressure losses

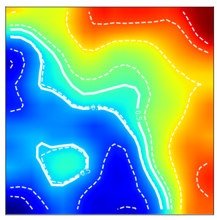

(b) Exit flow angle

Figure 14. Sensitivity of model for flow responses of the test cases

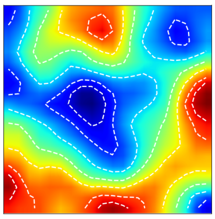

(a) Chordscale FB

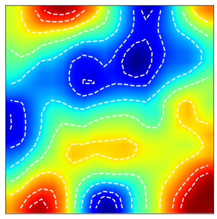

(b) Chordscale RB

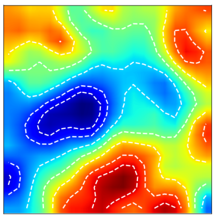

(c) LE FB

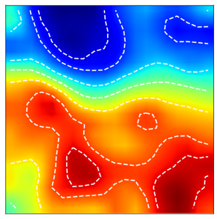

(d) LE RB

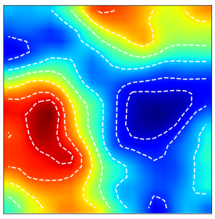

(e) PP

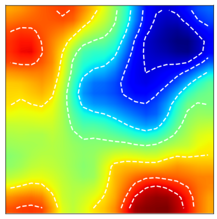

(f) AO

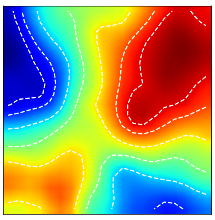

(g) Stagger FB

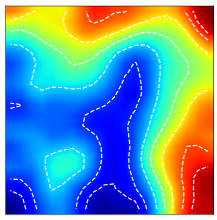

(h) Stagger RB

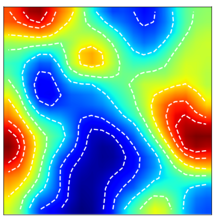

(i) TE FB

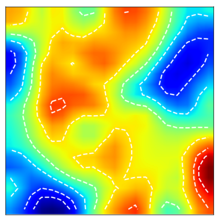

(j) TE RB

Figure 15. Sensitivity of model for flow inputs of the test cases

1.4 Range Optimization

The results of the second optimization are presented in this section.

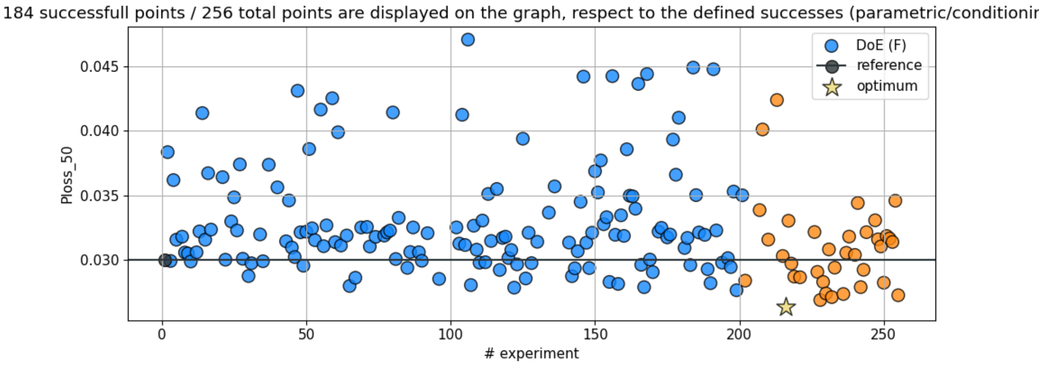

(a) Pressure losses

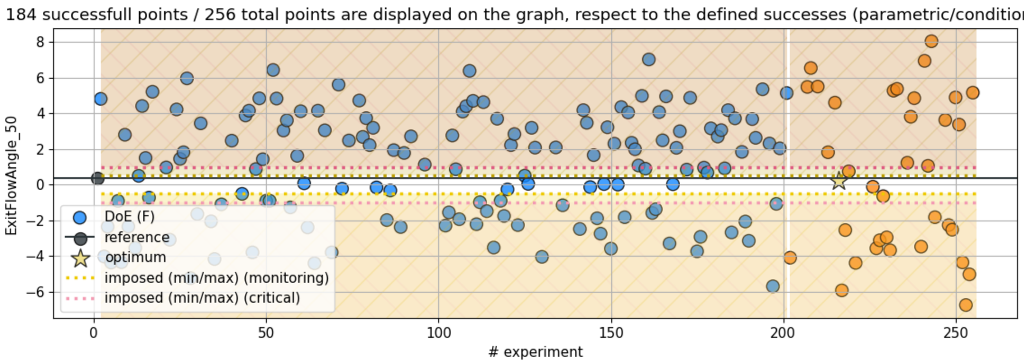

(b) Exit flow angle

Figure 16. Performance of flow quantities of the test cases

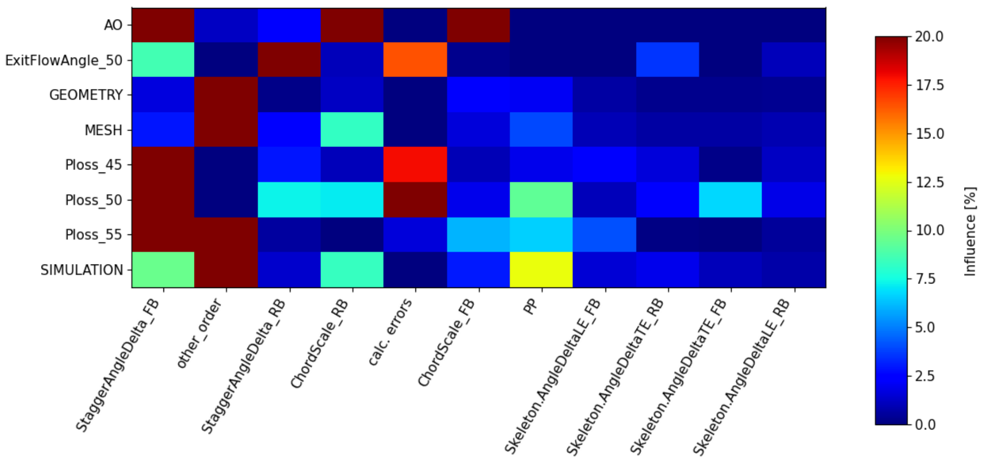

Figure 17. Global Sensitivity Analysis of the optimization

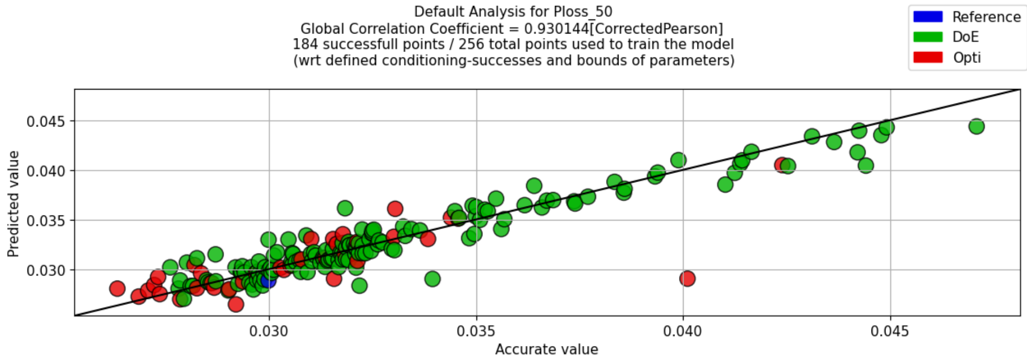

(a) Pressure losses

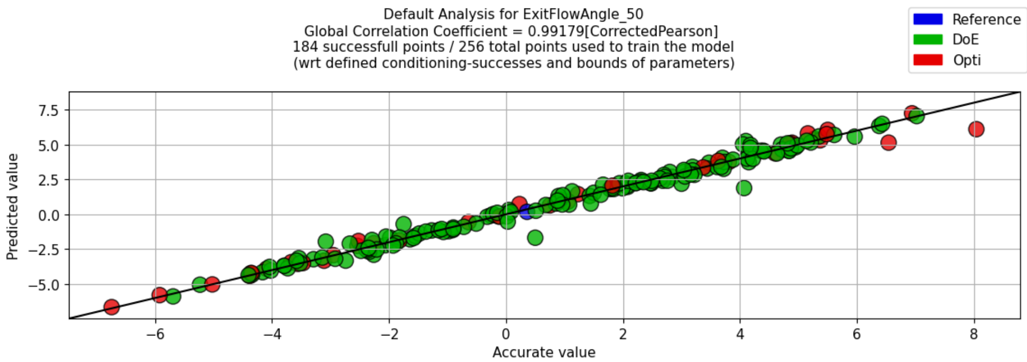

(b) Exit flow angle

Figure 18. Model quality of flow quantities of the test cases

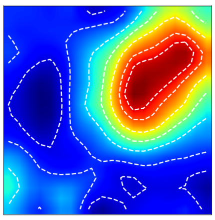

(a) Pressure losses

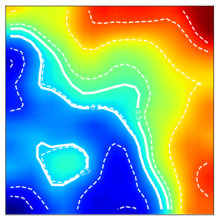

(b) Exit flow angle

Figure 19. Sensitivity of model for flow responses of the test cases

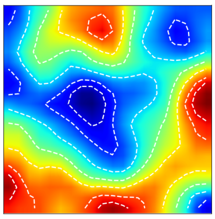

(a) Chordscale FB

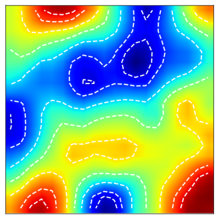

(b) Chordscale RB

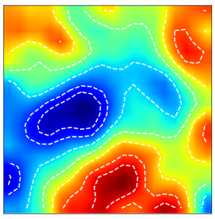

(c) LE FB

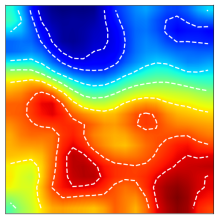

(d) LE RB

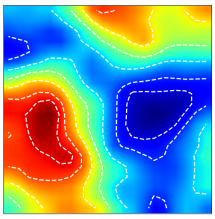

(e) PP

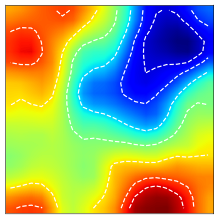

(f) AO

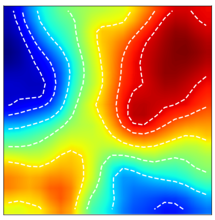

(g) Stagger FB

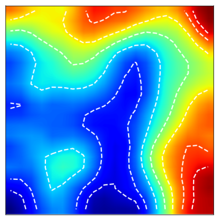

(h) Stagger RB

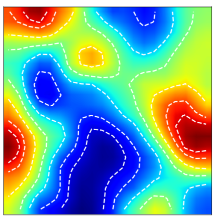

(i) TE FB

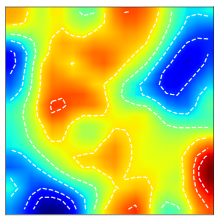

(j) TE RB

Figure 20. Sensitivity of model for flow inputs of the test cases

1.5 Upper Bound Optimization

The results of the last optimization are presented in this section.

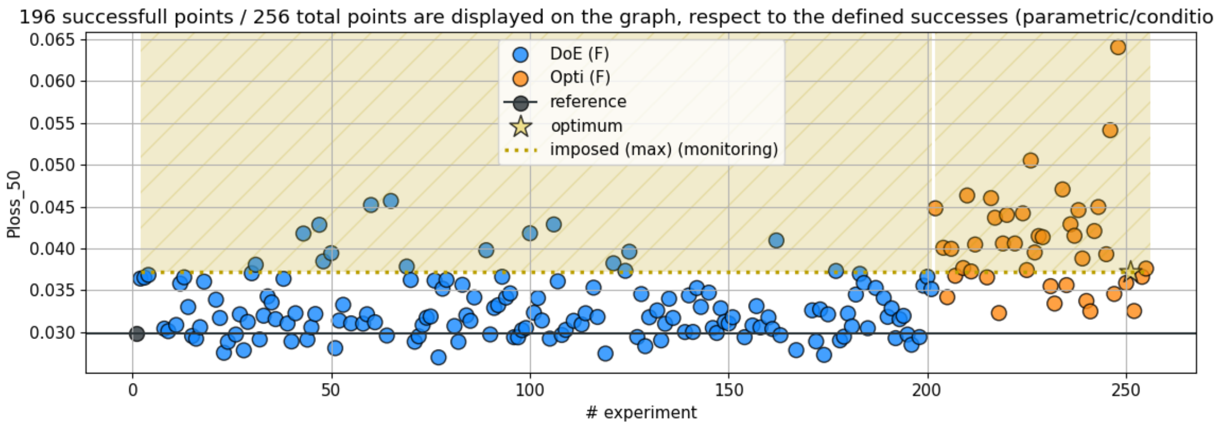

Figure 21. Pressure losses of the test cases

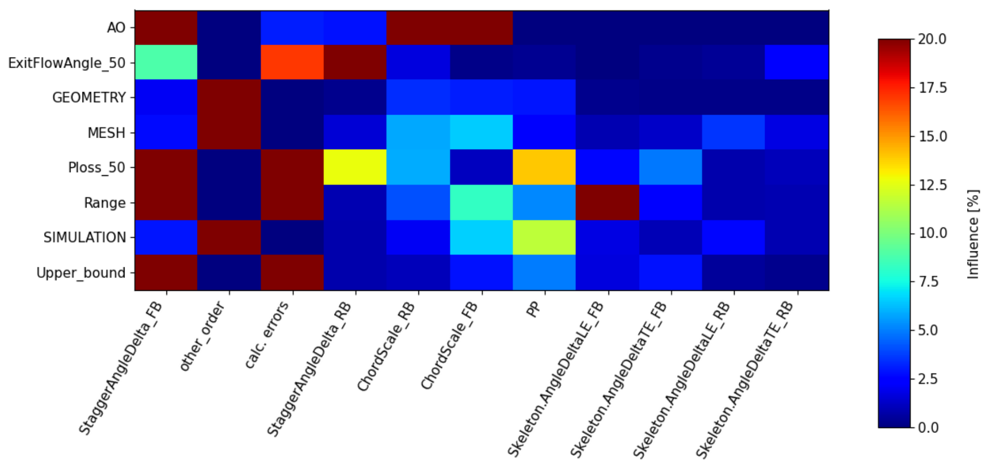

Figure 22. Global Sensitivity Analysis of the optimization

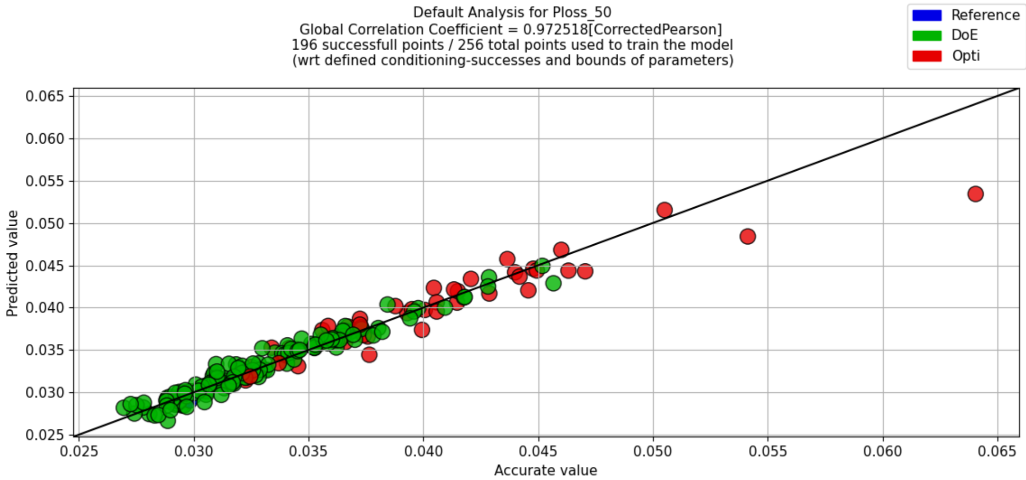

(a) Pressure losses

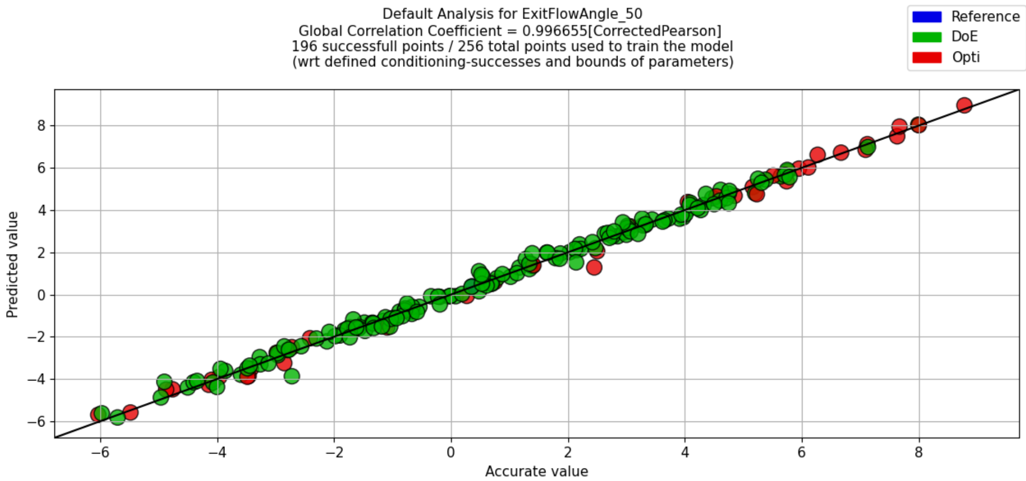

(b) Exit flow angle

Figure 23. Model quality of flow quantities of the test cases

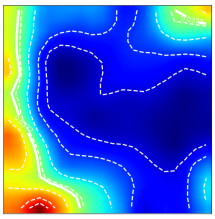

(**a**) Pressure losses

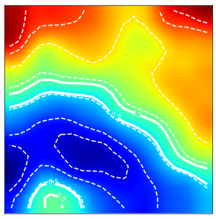

(**b**) Exit flow angle

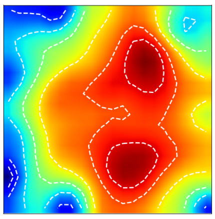

(**c**) Pressure losses

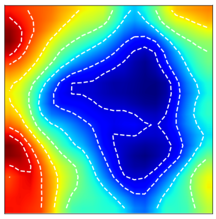

(**d**) Exit flow angle

Figure 24. Sensitivity of model for flow responses of the test cases

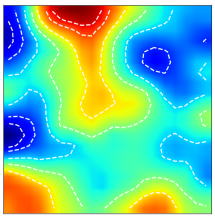

(a) Chordscale FB

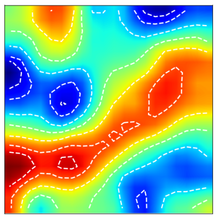

(b) Chordscale RB

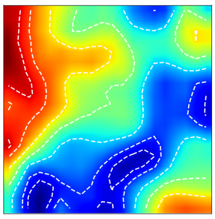

(c) LE FB

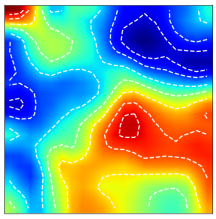

(d) LE RB

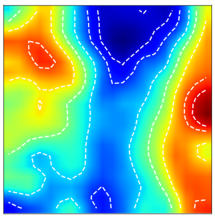

(e) PP

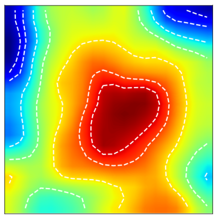

(f) AO

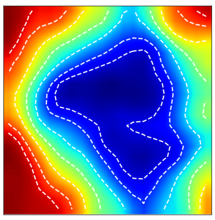

(g) Stagger FB

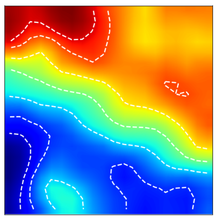

(h) Stagger RB

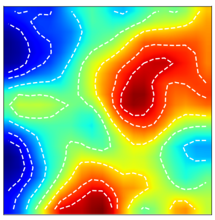

(i) TE FB

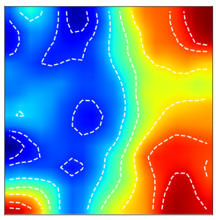

(j) TE RB

Figure 25. Sensitivity of model for flow inputs of the test cases